ELSEVIER

Brain Research Bulletin, Vol. 54, No. 3, pp. 267–273, 2001

0361-9230/01/$–see front matter

PII S0361-9230(00)00435-4

Interpreting PET and fMRI measures of functional neural activity: The effects of synaptic inhibition on cortical activation in human imaging studies

M.-A. Tagamets[1]* and Barry Horwitz[2]

[1]*Maryland Psychiatric Research Center, University of Maryland School of Medicine, Baltimore, MD, USA; and*
[2]*Voice, Speech and Language Branch, National Institute on Deafness and, Other Communication Disorders, National Institutes of Health, Bethesda, MD, USA*

[Accepted 26 October 2000]

ABSTRACT: Human brain imaging methods such as postiron emission tomography and functional magnetic resonance imaging have recently achieved widespread use in the study of both normal cognitive processes and neurological disorders. While many of these studies have begun to yield important insights into human brain function, the relationship between these measurements and the underlying neuronal activity is still not well understood. One open question is how neuronal inhibition is reflected in these imaging results. In this paper, we describe how large-scale modeling can be used to address this question. Specifically, we identify three factors that may play a role in how inhibition affects imaging results: (1) local connectivity; (2) context; and (3) type of inhibitory connection. Simulation results are presented that show how the interaction among these three factors can explain seemingly contradictory experimental results. The modeling suggests that neuronal inhibition can raise brain imaging measures if there is either low local excitatory recurrence or if the region is not otherwise being driven by excitation. Conversely, with high recurrence or actively driven excitation, inhibition can lower observed values. © 2001 Elsevier Science Inc.

KEY WORDS: Human brain imaging, Large-scale model, Inhibition, Local circuitry.

INTRODUCTION

Advances in human brain imaging methods such as positron emission tomography (PET) and functional magnetic resonance imaging (fMRI) have provided an unprecedented opportunity for studying the neural basis of human cognition. One unique feature of these techniques is that data can be obtained from essentially the entire brain simultaneously, thus providing a means for measuring widespread responses to cognitive tasks that are manipulated by the experimenter. Usually the goal of these studies is the localization of specific task components to particular brain areas [6,23]. More recently efforts have also been made to identify widespread functional networks that are characterized by different patterns of functional connectivity during different tasks [3,5,8,9,12,19,29]. Both of these approaches have begun to yield significant results, especially in the differentiation and separation of the components that make up a cognitive task. However, because imaging data is an indirect measure of neuronal activity, it has been difficult to relate the results of these studies to the underlying neuronal events, such as those measured during electrophysiological recordings in animals.

One question in particular has yet to be answered: Does neuronal inhibition, and the concomitant reduction in neuronal spiking activity, result in decreased measures in PET and fMRI? Activity measured in non-human animal studies by electrical recordings generally represents the firing of neurons (i.e., action potentials), whereas the hemodynamic-based measurements associated with PET and fMRI most likely reflect synaptic activity to a larger extent than neuronal activity [13,17]. PET and fMRI are hemodynamic/metabolic methods that are based on the notion that neural activity leads to an increase in both regional cerebral blood flow (rCBF) and brain oxidative metabolism [24,26]. Oxidative metabolism is thought to be needed to restore ionic concentrations following neural activity, with the greatest effects apparently occurring in the vicinity of synapses [17]. Because of this, it has been suggested that both excitatory and inhibitory synaptic activity might appear as increased PET or fMRI activity, even if the inhibition causes a decrease in overall local neuronal firing rates [10,13,18].

Most studies of excitatory neuronal effects have suggested that there is a direct relationship between spiking activity and oxidative metabolism. In autoradiography studies of the rat, stimulation of specific pathways has been shown to cause increases in local glucose metabolism at sites to which the stimulated location projects, but not where the stimulated spiking activity occurs [27]. The increases were proportional to the spiking rate of the stimulated neurons. Recent studies suggest that much of the metabolic activity that is measured in imaging data can be attributed to astrocytes, which mediate metabolic demands of the transmitter reuptake process at glutamatergic synapses [16]. This process appears to be very tightly coupled to the neuronal events. Since the

* Address for correspondence: M.-A. Tagamets, Maryland Psychiatric Research Center, University of Maryland School of Medicine, P.O. Box 21247, Baltimore, MD 21228, USA. Fax: +1-(410)-788-3394; E-mail: mtagamet@mprc.umaryland.edu

excitatory glutamatergic synapses are the most abundant in the neocortex, it is likely that this mechanism contributes the bulk of metabolic activity that is measured in PET and fMRI.

However, the role of inhibitory synapses in the observed data is still an open question. It has been suggested that a mechanism similar to that used at excitatory synapses underlies metabolic demands at inhibitory synapses [1,10,13]. Because these mechanisms require energy, inhibitory synaptic input might also be expected to increase metabolic activity. Electrical stimulation of known inhibitory pathways in the rat has been found to cause a rise in local glucose utilization at the site of the projections of these pathways [1]. More recently, Mathiesen et al. [18] measured both spiking activity in Purkinje neurons and local CBF simultaneously in the rat cerebellum during stimulation of either an excitatory or an inhibitory pathway. Comparable CBF increases were seen during both types of stimulation, even though inhibition reduced spiking activity in the Purkinje neurons. Based on these results, the authors concluded that it is impossible to determine if a rise in CBF reflects an increase or a decrease in spiking activity in the local neuronal population. On the other hand, rat autoradiography studies using agonists for the inhibitory neurotransmitter γ-aminobutyric acid (GABA) have generally shown decreases in measured energy metabolism [14,15,21]. Two human PET studies of the GABA agonist THIP have produced contradictory results. Roland and Friberg [25] showed a reduction of metabolism in most cortical regions following the administration of THIP, while Peyron et al. [22] found an increase.

The results summarized above suggest that it is difficult to make any direct interpretation of human brain imaging results in terms of the underlying neuronal activity when inhibition is present. However, there are likely to be specific factors that will allow us to gain some insight into these relationships. First, as several authors have noted (e.g., [18,21,28]), local circuit properties are likely to play a major role in determining the relationship between neuronal activity and measures such as rCBF. In the cortex, it is generally thought that the majority of connections occur within the confines of local circuitry, mostly within the range of neural assemblies such as cortical columns (e.g., [4]). Second, the response of a local circuit depends not only on its physical configuration, but also on the context in which the measurements are taken. For example, inhibitory stimulation of a circuit that is not otherwise engaged is likely to have a different effect from that observed when the circuit is actively being driven by another source. Thus, different task conditions might be expected to produce different local responses to inhibition, depending on the current state of the local circuit.

This is the type of problem that computational neuroscience methods may help address [2,10,11]. Recently, we [28] and others [2] have constructed large-scale, neurobiologically realistic computer models that contain multiple, interacting brain regions. In these models, neuroanatomical and electrophysiological data obtained from primate single cell recordings are used to simulate PET and fMRI data. These types of models thus provide a framework in which one can investigate how changes in the balance between excitatory and inhibitory synaptic activity could be reflected in PET/fMRI activity. In this paper, we use a single region of our model [28] to explore how the interaction of local circuits and task conditions can affect both spiking and blood flow measures. The central assumption used in the model is that changes in rCBF, glucose metabolism, and fMRI blood oxygenation (BOLD) measures are all primarily the result of local synaptic activity, whether excitatory or inhibitory.

OVERVIEW OF THE LARGE-SCALE NEURAL MODEL

The large-scale neural model we use [28] is made up of assemblies of local circuits that simulate various cortical areas along the ventral ("object") foveal vision pathway. The full-scale model is made up of areas V1/V2, V4, an inferior temporal (IT) area, and a prefrontal region that has been shown to be involved in working memory tasks involving object matching [7,20,31]. We have demonstrated that this model is able to perform a delayed match-to-sample task, while concurrently exhibiting electrical activities in each brain region that are similar to those seen in monkeys performing similar tasks, and local blood flow values that are comparable to those seen in human PET studies [28]. Recently, this model has been extended so that fMRI simulations can be conducted [11]. The use of large-scale neural models to simulate PET experiments was also reported by Arbib et al. [2] to examine a saccade generation task.

A key feature of the model is a basic local circuit that roughly corresponds to a cortical column. As shown in Fig. 1A, this circuit is a simple two-element (excitatory-inhibitory) unit that has local connection strengths that resemble the proportions suggested by anatomical studies [4]. The excitatory unit represents the assembly of pyramidal neurons in the column, while the inhibitory unit represents the inhibitory interneurons. The numbers on the arcs between elements in Fig. 1A represent relative synaptic efficacies, and they total to approximately 1. Thus, for example, the value 0.6 of the excitatory-to-excitatory connection can be viewed as representing about 60% of the total connections in the circuit. A more detailed description of the derivation of these values is given in Tagamets and Horwitz [28].

The equations that define the dynamic "electrical" behavior of the excitatory and inhibitory units are given in Eqs. 1 and 2, respectively:

$$\frac{dE_i(t)}{dt} = \Delta\left[\frac{1}{1 + e^{-K_E(in_{iE}(t) - \tau_E + N_E(t))}}\right] - \delta E_i(t) \quad (1)$$

$$\frac{dI_i(t)}{dt} = \Delta\left[\frac{1}{1 + e^{-K_I(in_{iI}(t) - \tau_I + N_I(t))}}\right] - \delta I_i(t) \quad (2)$$

where

$$in_{iE}(t) = \Sigma_j w^E_{ij} E_j(t) + \Sigma_j w^I_{ij} I_j(t) \text{ and } in_{iI}(t) = \Sigma_j w^E_{ji} E_j(t) + \Sigma_j w^I_{ji} I_j(t) \quad (3)$$

$E_i(t)$ and $I_i(t)$ represent the electrical activities of the excitatory (E) and inhibitory (I) elements, respectively, of unit i at time t. These values range between 0 and 1, and can be interpreted as reflecting percent of active units within a local population. The parameters K_E and K_I govern the reactiveness of the E and I elements to changes in incoming synaptic activity. τ_E and τ_I are the input thresholds, $N_E(t)$ and $N_I(t)$ are added noise terms, Δ is the rate of change, and δ is the decay rate.

$in_{iE}(t)$ and $in_{iI}(t)$ are the total synaptic inputs entering the excitatory and inhibitory elements of unit i at time t. These terms include inputs from within a unit itself as well as from other units. w^E_{ij} and w^I_{ij} are the synaptic efficacies coming from excitatory/inhibitory elements of unit j into unit i. The weights w^E_{ij} are positive-valued and the w^I_{ij} are negative-valued, reflecting the excitatory and inhibitory effects of each type of connection, respectively.

The PET/fMRI measure (which can represent rCBF or BOLD activity; for simplicity, we shall refer to it as rCBF) in the model is computed within an area as:

$$rCBF = \Sigma_{i,i,}(IN_i(t)) \quad (4)$$

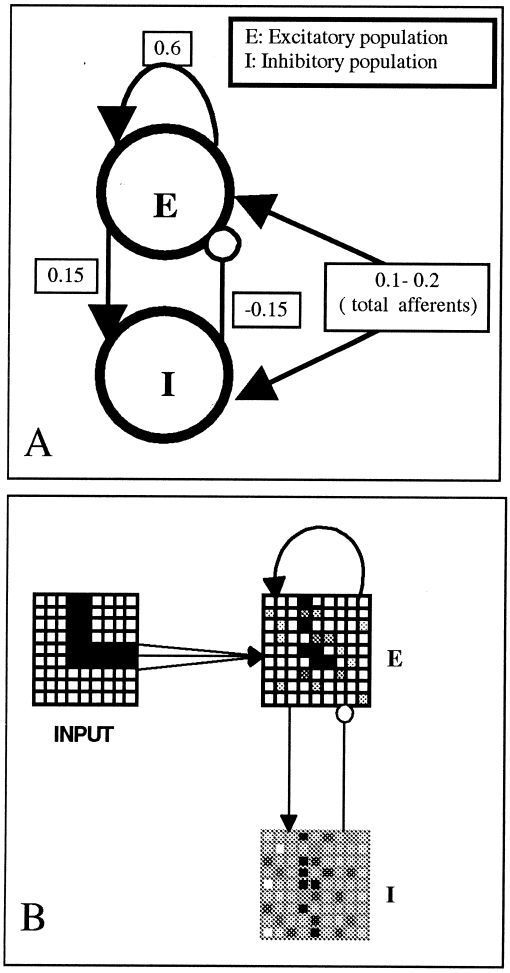

FIG. 1. The local circuit used in the model and a model brain region built up of local circuits. Excitatory synapses are shown by arrows, inhibitory by open circles. (A) The basic circuit has connection weights that are based on experimental data; 60% of all connections are local and excitatory-to-excitatory, 15% are local excitatory-to-inhibitory, 15% are local inhibitory-to-excitatory, and the remaining 10% are from other areas. (B) Basic circuits are grouped into topographically organized 9 × 9 arrays.

$IN_i(t)$ is the sum of absolute values of the inputs to both the *E* and *I* elements of unit *i*, both from within the unit and from all sources, at time *t*, and is computed as:

$$IN_i(t) = \Sigma_{k,i} w_{ki} E_k(t) + \Sigma_{m,i} |w_{mi}| I_m(t) \quad (5)$$

In Eq. 4 the absolute synaptic activity is integrated over the time course for the study (e.g., approximately 1 min for rCBF-PET and about 50–100 ms for BOLD-fMRI). This is similar to the method used in [2] for computing simulated blood flow.

The basic units are assembled into a 9 × 9 array, A, which represents approximately a 1-cm^2 patch of cortex, as shown on the right in Fig. 1B. Another 9 × 9 array, shown on the left in Fig. 1B, acts as an input to the cortical array. There are weighted connections from the input array into the cortical patch, so that any activity that is present in the input is transmitted to area A. During simulations a subset of units in the input are clamped to a fixed value in order to simulate a patterned input. Activations are passed from the input to the cortical area, where they are integrated by the Eqs. 1 and 2 to yield electrical activity patterns over time. In order to simulate PET data, the absolute values of all synaptic activities in the cortical region are summed according to Eq. 4.

SIMULATIONS: EXCITATION, INHIBITION AND PET ACTIVITY

An important property of the connectivity pattern in the basic circuit is that most connections are local and excitatory (see Fig. 1A). This fact might at first suggest that local blood flow (synaptic activity) is dominated by the state of the excitatory units in a local region. If this were indeed the case, one would expect that any afferent inhibition would decrease blood flow, because the local activity of the pyramidal neurons is decreased. However, both the experimental studies cited earlier and our modeling studies indicate that this is not necessarily true. Our modeling studies suggest that there may be different effects, depending on three main factors: (1) type of afferent; (2) context, or task; and (3) local cortical connectivity. In the following we present simulations that demonstrate how each of these factors can affect measured PET activation.

Effects of Afferent Type and Task in the Model Circuit

First we examine the responses (both spiking frequency and simulated PET) of the local region A to four different types of input. Region A receives inputs from two separate sources simultaneously. For simplicity, we refer to the inputs depicted on the left in Fig. 2 as the *context* and the inputs depicted by the ovals on the right side as the *afferent* input. A configuration like this is typical in the cortex, in which all regions are connected to multiple other regions. Thus, for example, some regions receive high levels of excitation during sensory input (the context) while simultaneously receiving modulatory afferents (either excitatory or inhibitory) from other regions. Recall that the excitatory (*E*) units in the model correspond to cells such as pyramidals, whose spiking activity is typically measured in electrophysiological experiments.

In any given context, afferent excitation of the *E* units can occur in one of two ways: (1) directly, by synapses directly on the *E* units (Fig. 2, case A), or, (2) indirectly, by inhibition of the local inhibitory (*I*) units (case B). Likewise, inhibition can occur either (1) directly, by inhibitory synapses on the *E* units (case C), or, (2) indirectly, by excitation of the *I* units (case D). These four cases are illustrated by the oval afferents to the right of the model regions in Fig. 2. Context is provided from the inputs shown on the left. An "active" context is simulated by presenting shaped patterns with high activity to the input area. A resting or passive context is simulated by setting all units in the input region to a uniformly low value. The latter reflects a case in which area A does not receive inputs from any other source. In order to examine afferent effects in these different contexts, the four types of afferents depicted in Fig. 2 were simulated during each of two task conditions: (1) a low baseline (resting) condition, and (2) with a high level of input coming from the input region. Simulations for each case are run for 200 iterations, with each iteration corresponding to approximately 5 ms of time.

Figure 3 shows the results of these simulations. Both simulated CBF (solid lines) and the mean spiking levels in the region (dashed lines –o–) are depicted in the graphs of Fig. 3. The upper pairs of curves (beginning at y = 0.4) in each graph are the high context (active) condition, and the lower two curves (starting at y = 0.2) depict the baseline context, when there is no other activity entering the region. Along each curve, the context input is held constant, while the afferents are systematically increased. The x-axis represents increasing afferent input coming from the oval sources in Fig. 2. Figure 3A and B show the two cases in which the net effect

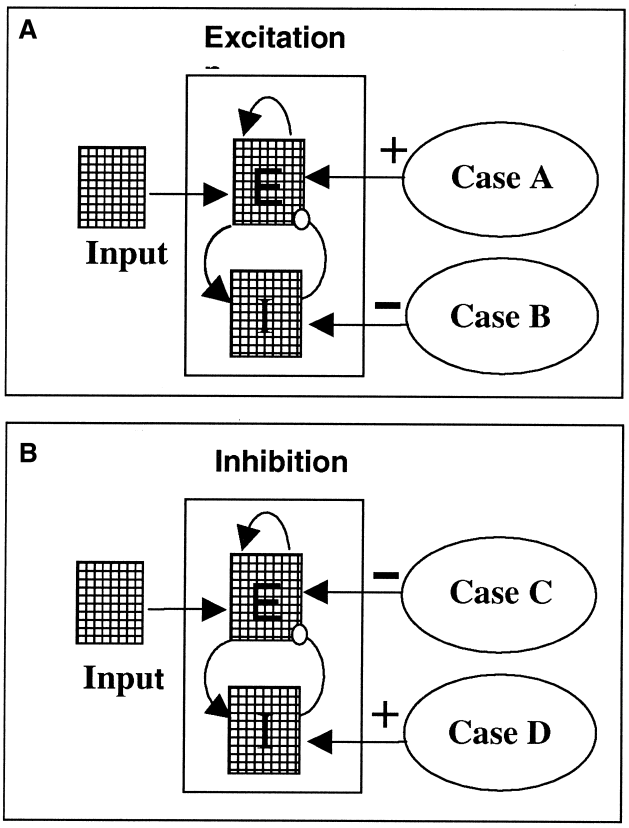

FIG. 2. Four different types of afferents to a region. An input area (shown to the left of each local region) provides context, such as that experienced during sensory stimulation, for example. Connections from the input area on the left of each figure are topographically arranged and are all excitatory. Different types of excitatory and inhibitory afferents are shown on the right in ovals. The afferent connections are weak and synapse onto all units equally. (A) Two types of excitatory effects: Excitation by excitatory-to-excitatory connections (case A) and indirect excitation of the excitatory units by inhibitory-to-inhibitory afferents (case B). (B) Two types of inhibitory effects: Direct inhibition by inhibitory-to-excitatory connections (case C) and indirect inhibition by excitatory-to-inhibitory afferents (case D).

is excitation of the *E* units, and correspond to the cases shown in Fig. 2, case A and case B, respectively. In both cases, the electrical activity and the CBF measure both rise more or less concurrently with rising afferent modulation. This is consistent with the excitatory effects observed in animal studies [18,27]. Figure 3C and D depict the two inhibitory cases. In the task context (upper curves), when there is a high level of activity coming from other regions, both spiking and CBF decline with increasing afferent inhibition, although there tends to be a relatively greater drop in spiking than in the CBF as the inhibitory effect is increased. In the baseline conditions (lower curves of each graph), there is a dissociation between the modeled spiking activity, which drops, and the CBF, which rises. This effect is particularly notable in the indirect inhibitory case, in which inhibition is achieved by excitatory afferent inputs to the *I* units. The latter mechanism corresponds to the indirect inhibitory pathway experimental condition in the study of Mathiesen et al. [18], in which reduction of spiking in the Purkinje cells results from an indirect pathway through inhibitory neurons. The simulated results suggest that when a region does not receive extensive excitation from other sources, and given the local circuit properties shown in Fig. 1A, synaptic activity from afferent inhibition can exceed total reduction of local synaptic activity. The result is a rise in CBF, even though spiking is reduced in local *E* neurons.

Effects of Local Connectivity and Afferents

Interpreting imaging data also depends on the question: how does structure of the local circuit influence measured PET or fMRI data. In the previous example, the local circuit was fixed, while afferent strengths were modified. The connectivity strengths used in the basic circuit of our model (Fig. 1A) are based on data from normal cortical tissue. There are likely to be differences among different cortical regions, as well as in subcortical areas and in certain disease states. If local circuits are not dominated by local excitatory recurrence, how would inhibitory effects be expressed in measures of PET and fMRI? At the two extremes of recurrent connectivity strength, a local circuit could either have no local connections at all, or else virtually all connections could be local. In the former, with no local connectivity, all synapses are from an external source, and any afferent inhibition would raise local synaptic activity. At the other extreme, if almost all activity is local, afferents are swamped by the local response, and CBF would reflect mainly the local activity. The question then arises, how does the relation between spiking and CBF change along the continuum between these two extremes? To examine this issue we used the model region A for examining how the magnitude of local recurrent excitation, in a range between the two extremes, can affect computed rCBF. Various recurrent connection strengths in this range are examined under two different levels of context, which correspond to a task and a control condition, as in the previous section. Simulations were again performed by presenting a pattern to the inputs that project to the excitatory population of the area and computing rCBF for the duration of the stimulus. Afferent inhibition was implemented as a low level of excitation to all of the local inhibitory units in area A, such as shown in case D of Figs. 2 and 3. Simulations and computation of PET were implemented as before.

Figure 4 shows the computed PET activity from the simulations for each of the conditions as local recurrent excitation increases. Active context conditions are shown in Fig. 4A and baseline in 4B. Solid lines represent simulated PET with no additional afferent inhibition and dashed lines are PET values in the presence of additional afferent inhibition. The x-axis represents excitatory-to-excitatory connection strength within the basic circuits of the area, i.e., the value of the *E*-to-*E* connection strength. Again, context stimulation was held constant for all points along each graph.

It can be seen by the rise in all curves that increasing local recurrent excitation increases the local CBF response in all cases, as would be expected. Note that all context inputs, both excitatory and inhibitory, are the same for all points along a curve. The only difference is the amount of local recurrent excitation, which increases along the x-direction. At low levels of local feedback excitation, below about 0.5 along the x-axis, both the high (task) and low (baseline) context conditions show a higher CBF in the presence of inhibition (dashed lines) than without inhibition (solid lines). At higher levels of recurrent local excitation, the relationship changes in the task condition, so that the inhibited case (dashed curve) has lower computed rCBF than the case without inhibition (solid line), but the baseline condition shows the opposite effect. At very high recurrent levels, beyond about 0.7, inhibition produces lower simulated PET in both task and baseline conditions. In the regime thought to correspond to the amount of recurrence in the cortex (the region between the dark vertical lines in Fig. 4, corresponding to *E*-to-*E* connection strengths of 0.5–0.7), afferent inhibition has opposite effects in baseline and task

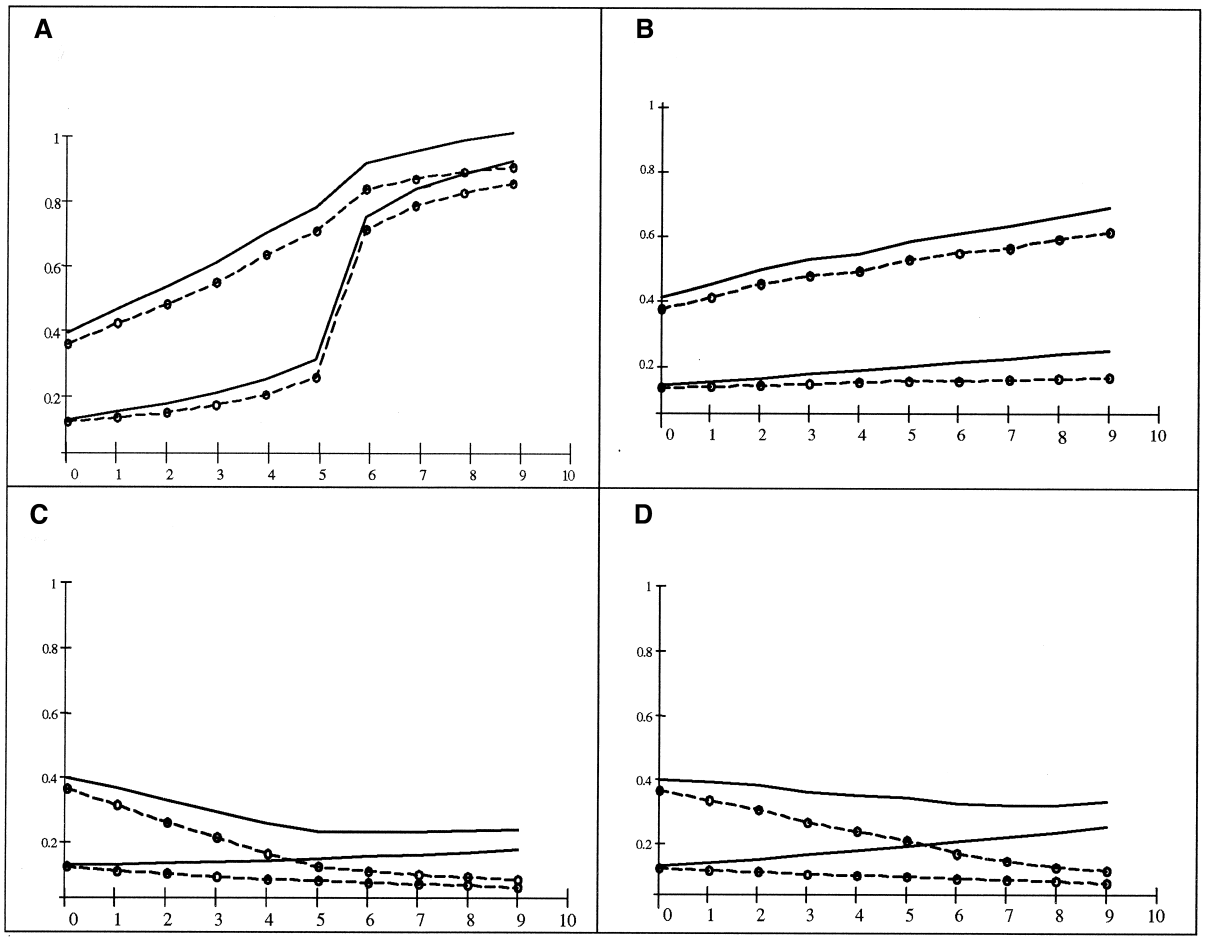

FIG. 3. Electrical activity (—o—) and simulated cerebral blood flow (CBF) activity (solid lines) that result from the different afferent input types shown in Fig. 2. For each case, the amount of afferent excitation or inhibition (ovals to the right of the networks in Fig. 2) was systematically increased, as shown along the x-axis. Mean electrical activity and mean CBF activity was computed for the combined *E–I* grouping that represents the local cortical region. (A), (B) Result of excitation, corresponding to case A and case B, respectively, in Fig. 2A. (C), (D) Inhibitory effects, corresponding to Fig. 2B, case C and case D, respectively.

conditions. While the exact crossover points will vary, depending on the specific levels of baseline and active activations, the point is that crossover always occurs earlier in a more activated context than in a less activated context.

DISCUSSION

We have used computational modeling to examine factors that potentially play a role in the relationship between neuronal events and the signals measured in human brain imaging experiments. Although experimental studies indicate that there is a close correlation between neuronal excitation and imaging measures such as metabolism/CBF, the same can not be said for neuronal inhibition. Specifically, experimental results examining the relation between inhibition and CBF/metabolism have been inconclusive, or have suggested that it is not possible to distinguish between excitation and inhibition in CBF measures. Our modeling studies suggest that there may be factors which, when taken into account, can aid in the interpretation of imaging results. Specifically, we have examined three separate components that are likely to play a role in how neuronal inhibition may be reflected by metabolism/blood flow measurements. First, the type of inhibitory connection, whether direct or indirect, had somewhat different effects, in that indirect inhibitory connections caused a relatively greater rise in CBF than did direct connections. The pathway used in the study by Mathiesen et al. [18] was indirect, via inhibitory interneurons, with the result that they observed a large CBF increase even though the excitatory neurons in the region had reduced levels of spiking. Second, the context in which inhibition occurs may play a role. The modeling suggests that, given a moderate to high recurrent excitatory local connectivity, inhibition is more likely to result in increases of CBF/metabolism in a context where the region does not receive excitation from other sources. Third, the amount of local excitatory recurrence determines whether metabolism/CBF reflects mainly local or mainly afferent synaptic activity. Anatomical studies suggest that recurrence in local cortical circuits is in the range in which our model suggests there inhibition may cause opposite effects between high and low activity contexts. While the exact amount of recurrence in different cortical areas is not known, our model nevertheless suggests that under conditions that are similar to those found in cortical circuits, it is possible that the net effect of inhibition on imaging results can depend on the nature of the task comparisons in subtle ways.

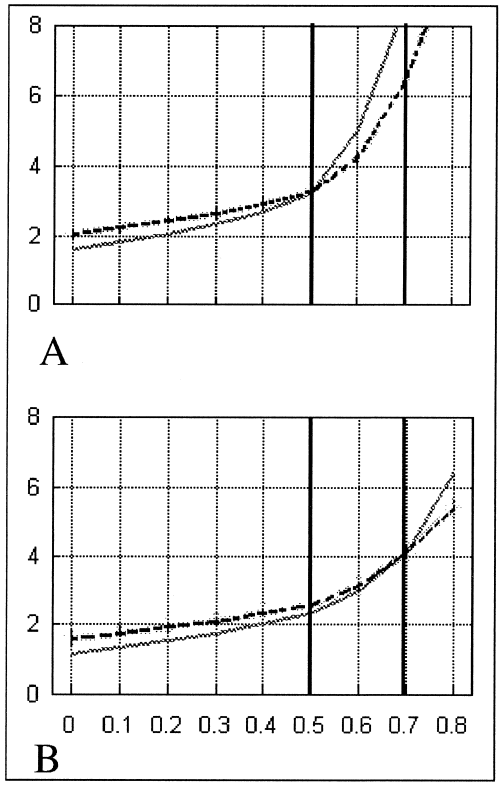

FIG. 4. The effects of increasing local recurrent connectivity. Solid curves show the modeled positron emission tomography (PET) activity without any added inhibition. Dashed curves show computed PET with afferent inhibition. (A) High context level, such as in an active task condition, in which there is a moderately high extrinsic signal arriving into the area. (B) A low context condition, in which most activity is intrinsic, such as during a baseline resting condition.

Experimental methods could be used to examine these issues in the future. The experimental system used by Mathiesen et al. in [18] might be one useful approach. They stimulated climbing fibers, which have monosynaptic excitatory connections to Purkinje cells, and parallel fibers, which have an indirect inhibitory effect. However, each of these conditions was tested separately. The relationships suggested by our simulations could be tested directly by varying the amounts of both excitation and inhibition through each of these pathways. The model would predict that if one begins with a highly excited state, and then applies inhibition via the parallel pathway, CBF would go down, relative to the excited state. Because most imaging studies generally examine differences between states, a better understanding of these issues will help clarify interpretation of the results obtained from functional neuroimaging studies.

In contrast to experiments that used electrical stimulation via natural inhibitory pathways [1,18], studies using agonists for the inhibitory neurotransmitter GABA have generally reported decreases in CBF/metabolism in association with neuronal inhibition [14,15,25]. However, metabolic demands are thought to be mainly presynaptic [16], while GABA agonists such as THIP work postsynaptically. Thus, the results of these drug studies are what would be expected.

These considerations are especially relevant to the understanding of imaging results from patient populations. The effects of focal lesions, in which whole populations of columns are removed, are likely to be quite different from those that result from more diffuse degenerative processes, where local connectivity is reduced, or from disconnection between areas, in which local circuitry may remain unchanged but total afferents are reduced. As an example of the case in which local circuits are compromised, Alzheimer's disease is characterized by a loss of large pyramidal neurons in layers 3 and 5 [30], leading to an excess of inhibitory neurons relative to excitatory neurons. Issues such as those examined here need to be explored in more detail before definitive interpretation of the neuronal dynamics underlying PET and fMRI data is possible.

REFERENCES

1. Ackermann, R. F.; Finch, D. M.; Babb, T. L.; Engel, J. Jr. Increased glucose metabolism during long-duration recurrent inhibition of hippocampal pyramidal cells. J. Neurosci. 4:251–264; 1984.
2. Arbib, M. A.; Bischoff, A.; Fagg, A. H.; Grafton, S. T. Synthetic PET: Analyzing large-scale properties of neural networks. Hum. Brain Mapp. 2:225–233; 1995.
3. Buechel, C.; Friston, K. J. Modulation of connectivity in visual pathways by attention: Cortical interactions evaluated with structural equation modeling and FMRI. Cereb. Cortex 7:768–778; 1997.
4. Douglas, R. J.; Koch, C.; Mahowald, M.; Martin, K. A.; Suarez, H. H. Recurrent excitation in neocortical circuits. Science 269:981–985; 1995.
5. Friston, K. J. Functional and effective connectivity in neuroimaging: A synthesis. Hum. Brain Mapp. 2:56–78; 1994.
6. Friston, K. J.; Holmes, A. P.; Worsley, K. J.; Poline, J. P.; Frith, C. D.; Frackowiak, R. S. J. Statistical parametric maps in functional imaging: A general linear approach. Hum. Brain Mapp. 2:189–210; 1995.
7. Haxby, J. V.; Ungerleider, L. G.; Horwitz, B.; Rapoport, S. I.; Grady, C. L. Hemispheric differences in neural systems for face working memory: A PET-RCBF study. Hum. Brain Mapp. 3:68–82; 1995.
8. Horwitz, B. Data analysis paradigms for metabolic-flow data: Combining neural modeling and functional neuroimaging. Hum. Brain Mapp. 2:112–122; 1994.
9. Horwitz, B.; Grady, C. L.; Haxby, J. V.; Ungerleider, L. G.; Schapiro, M. B.; Mishkin, M.; Rapoport, S. I. Functional associations among human posterior extrastriate brain regions during object and spatial vision. J. Cogn. Neurosci. 4:311–322; 1992.
10. Horwitz, B.; Sporns, O. Neural modeling and functional neuroimaging. Hum. Brain Mapp. 1:269–283; 1994.
11. Horwitz, B.; Tagamets, M. A. Predicting human functional maps with neural net modeling. Hum. Brain Mapp. 8:137–142; 1999.
12. Horwitz, B.; Tagamets, M. A.; McIntosh, A. R. Neural modeling, functional brain imaging and cognition. Trends Cogn. Sci. 3:91–98; 1999.
13. Jueptner, M.; Weiller, C. Review: Does measurement of regional cerebral blood flow reflect synaptic activity? Implications for PET and FMRI. Neuroimage 2:148–156; 1995.
14. Kelly, P. A.; Ford, I.; McCulloch, J. The effect of diazepam upon local cerebral glucose use in the conscious rat. Neuroscience 19:257–265; 1986.
15. Kelly, P. A.; McCulloch, J. Effects of the putative GABAergic agonists, muscimol and THIP, upon local cerebral glucose utilisation. J. Neurochem. 39:613–624; 1982.
16. Magistretti, P. J.; Pellerin, L. Cellular mechanisms of brain energy metabolism and their relevance to functional brain imaging. Philos. Trans. R. Soc. Lond. B Biol. Sci. 354:1155–1163; 1999.
17. Mata, M.; Fink, D. J.; Gainer, H.; Smith, C. B.; Davidsen, L.; Savaki, H.; Schwartz, W. J.; Sokoloff, L. Activity-dependent energy metabolism in rat posterior pituitary primarily reflects sodium pump activity. J. Neurochem. 34:213–215; 1980.
18. Mathiesen, C.; Caesar, K.; Akgoren, N.; Lauritzen, M. Modification of activity-dependent increases of cerebral blood flow by excitatory synaptic activity and spikes in rat cerebellar cortex. J. Physiol. (Lond.) 512(Pt. 2):555–566; 1998.

19. McIntosh, A. R.; Grady, C. L.; Ungerleider, L. G.; Haxby, J. V.; Rapoport, S. I.; Horwitz, B. Network analysis of cortical visual pathways mapped with PET. J. Neurosci. 14:655–666; 1994.
20. Miller, E. K.; Erickson, C. A.; Desimone, R. Neural mechanisms of visual working memory in prefrontal cortex of the macaque. J. Neurosci. 16:5154–5167; 1996.
21. Palacios, J. M.; Kuhar, M. J.; Rapoport, S. I.; London, E. D. Effects of gamma-aminobutyric acid agonist and antagonist drugs on local cerebral glucose utilization. J. Neurosci. 2:853–860; 1982.
22. Peyron, R.; Le Bars, D.; Cinotti, L.; Garcia-Larrea, L.; Galy, G.; Landais, P.; Millet, P.; Lavenne, F.; Froment, J. C.; Krogsgaard-Larsen, P. Effects of GABAA receptors activation on brain glucose metabolism in normal subjects and temporal lobe epilepsy (TLE) patients. A positron emission tomography (PET) study. Part I: Brain glucose metabolism is increased after GABAA receptors activation. Epilepsy Res. 19:45–54; 1994.
23. Posner, M. I.; Petersen, S. E.; Fox, P. T.; Raichle, M. E. Localization of cognitive operations in the human brain. Science 240:1627–1631; 1988.
24. Roland, P. E. Brain activation. New York: Wiley-Liss; 1993.
25. Roland, P. E.; Friberg, L. The effect of the GABA-A agonist THIP on regional cortical blood flow in humans. A new test of hemispheric dominance. J. Cereb. Blood Flow Metab. 8:314–323; 1988.
26. Siesjo, B. K. Brain energy metabolism and catecholaminergic activity in hypoxia, hypercapnia and ischemia. J. Neural Transm. 14(suppl.): 17–22; 1978.
27. Sokoloff, L. Sites and mechanisms of function-related changes in energy metabolism in the nervous system. Dev. Neurosci. 15:194–206; 1993.
28. Tagamets, M. A.; Horwitz, B. Integrating electrophysiological and anatomical experimental data to create a large-scale model that simulates a delayed match-to-sample human brain imaging study. Cereb. Cortex 8:310–320; 1998.
29. Taylor, J. G.; Krause, B.; Shah, N. J.; Horwitz, B.; Mueller-Gaertner, H. W. On the relation between brain images and brain neural networks. Hum. Brain Mapp. 9:165–182; 2000.
30. Terry, R. D.; Peck, A.; DeTeresa, R.; Schechter, R.; Horoupian, D. S. Some morphometric aspects of the brain in senile dementia of the Alzheimer type. Ann. Neurol. 10:184–192; 1981.
31. Wilson, F. A.; Scalaidhe, S. P.; Goldman-Rakic, P. S. Dissociation of object and spatial processing domains in primate prefrontal cortex [see comments]. Science 260:1955–1958; 1993.